

Dense, layered, inclined flows of spheres

James T. Jenkins*

School of Civil and Environmental Engineering, Cornell University, Ithaca, New York 14853, USA

Michele Larcher†

Faculty of Science and Technology, Free University of Bozen-Bolzano, 39100 Bozen-Bolzano, Italy

(Received 13 April 2017; published 20 December 2017)

We consider dense, inclined flows of spheres in which the particles translate in layers, whose existence may be promoted by the presence of a rigid base and/or sidewalls. We imagine that in such flows a sphere of a layer is forced up the back of a sphere of the layer below, lifting a column of spheres above it, and then falls down the front of the lower sphere, until it bumps against the preceding sphere of the lower layer. We calculate the forces and rate of momentum transfer associated with this process of rub, lift, fall, and bump and determine a relation between the ratio of shear stress to normal stress and the rate of strain that may be integrated to obtain the velocity profile. The fall of a sphere and that of the column above it results in a linear increase in the magnitude of the velocity fluctuations with distance from the base of the flow. We compare the predictions of the model with measured profiles of velocity and granular temperature in several different dense, inclined flows.

DOI: [10.1103/PhysRevFluids.2.124301](https://doi.org/10.1103/PhysRevFluids.2.124301)**I. INTRODUCTION**

Slow dense flows of granular materials down inclines occur in many industrial processes and are common in nature. However, the understanding of such flows is still incomplete. Physical experiments on inclined flows [1–10] have illuminated the gross features of such flows. They have also led to scalings that describe some features and the interpretation of these features in terms of their micromechanical origins. Experiments in two dimensions on a rigid, bumpy base [11–14], in which the particles are confined between parallel walls separated by a distance slightly more than a sphere diameter, have provided access to the interior of the flow at the expense of introducing side walls. Recent advancements in techniques based on refractive index matching provide the opportunity to study similar features inside three-dimensional flows, at least for fluid-particle mixtures (e.g., Refs. [15,16]), without the limitation of focusing only on the near-wall particles (e.g., Refs. [17,18]).

The results of numerical simulations [2,13,19–28] give a wealth of information on both the gross features and the details of particle interaction and structure. This information provides the basis for more detailed description of the rheology.

The μ - I rheology [7,8] is an example of a simple, successful description of dense, steady, homogeneous shearing flow that has also been applied with some success to inhomogeneous and unsteady flows. It employs I , the inertial number, a dimensionless measure of the time associated with the product of the particle diameter and shear rate to a time associated with the pressure normalized by the mass density of the material of the particles: $I = du'/(p/\rho_s)^{1/2}$. It relates I to the ratio, μ , of the shear to the pressure:

$$\mu(I) = \mu_s + \frac{\mu_g - \mu_s}{I_0 + I} I, \quad (1)$$

*jim.jenkins@cornell.edu

†michele.larcher@unibz.it

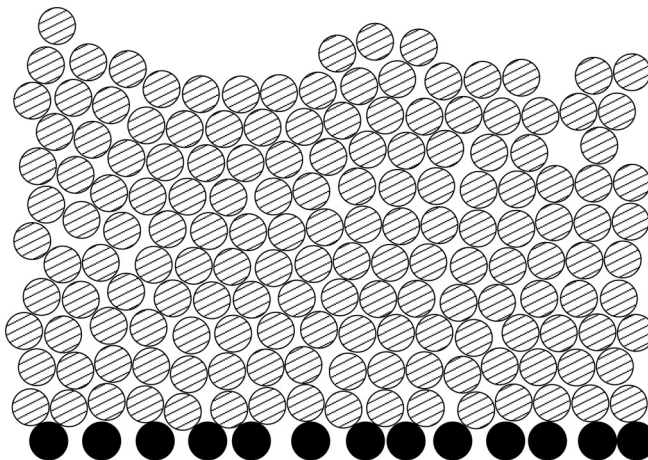


FIG. 1. Sketch of 2D flow of spherical beads down a bumpy incline, comprising spheres (black) fixed to the bed of the flume.

where μ_g , μ_s , and I_0 are parameters in the model. The observations of columns of particles in the experiments and simulations have inspired unique, explicitly nonlocal phenomenological theories [29,30]. References [31,32] provide an extension of the GDR MiDi [7] rheology that incorporates nonlocality through the spatial gradients.

Jenkins and Berzi [33] place an extension of the kinetic theory for shearing flows with correlated collisions in the context of the μ - I rheology. This is important to us, because the μ - I modeling says nothing about the strength of the particle velocity fluctuations. However, in kinetic theories for particle segregation (e.g., Refs. [34,35]), gradients in the strength of the particle velocity fluctuations provide an important segregation mechanism. In dense, collisional inclined flows over a rigid, bumpy base, Jenkins and Berzi [33] indicate that the strength of the velocity fluctuations decreases from the base to the top of the flow. However, discrete numerical simulations and physical experiments on other inclined flows over rigid and erodible beds indicate that there are situations in which the particle velocity fluctuations increase linearly in strength from the base of the flow (i.e., those of Sec. III). The model that we propose may be interpreted as a nonlocal extension of the μ - I rheology, in which both enduring particle contacts and collisions play a role and which has the capacity to say something about the increase in the strength of the velocity fluctuations with distance from the base.

In this paper, we first consider a dense, dry, plane inclined flow of identical, frictional spheres over a rigid, bumpy, frictional base. For simplicity, we assume that the base is composed of equally spaced spheres that are identical to those of the flow. We are interested in predicting the profiles of the average velocity and the strength of the velocity fluctuations and the relationship between the mean velocity of the flow and its depth. We also wish to determine how the inclination of the flow, the spacing of the particles, and the coefficient of friction of the particles influence these features.

In doing so, we describe granular flows in which the force chains extend from the interior to the base, extending the limits of validity of the extended kinetic theory [33,36,37]. Moreover we can include the nonlocal effects created by ephemeral networks of sliding contacts; the importance of these has been pointed out [38–42]. Such networks are important also in the context of geophysical flows (e.g., Ref. [43]).

The modeling also incorporates the layering seen in physical experiments and numerical simulations of slow dense flows [13,20,21,27,44] that indicate that at least in the neighborhood of the base the particles are aligned in layers, parallel to the base, that move relative to each other (see Fig. 1). Individual particles in neighboring layers interact through sliding and bumping. Frictional resistance at sliding contacts may also contribute to the component of force parallel

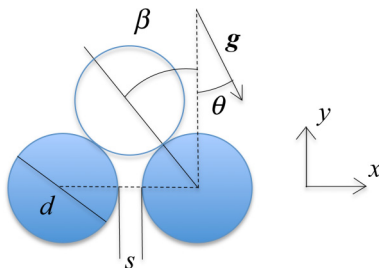


FIG. 2. The penetration of a sphere into the layer below showing the largest angle β between the line of centers and the normal to the flow. The angle of the flow to the horizontal is θ .

to the flow. The rate of momentum exchanged between bumping particles provides an additional contribution. A similar organization in ordered layers is observed also in dry flows within rotating tumblers [45–49] and in fluid-saturated, gravity-driven granular flows over erodible beds, using both spherical particles [50,51] and quasispherical, cylindrical particles [52–54]. Given this, we employ the layered rheology even in the absence of a base.

Our assumption regarding the interaction between the particles in two adjacent layers is that a particle in the upper layer first slides up the back surface of a particle in the layer below; after reaching the highest point on the lower particle, it falls under gravity down the front surface of the lower particle and bumps into the particle ahead of it. The frequency, f , of the bumps experienced by a particle in the lower layer is proportional to the difference in the average flow velocity of the layers and inversely proportional to the distance between the layers, which we assume to be equal to the particle diameter, d . As a consequence, we take $f = u'$, which is the y derivative of the average flow velocity u .

In such a dense flow, each particle supports the weight of the particles above it through an ever-changing network of sliding contacts. For this reason, we assume that during the sliding and bumping, each grain supports the weight of the column of particles above it, until it falls down the front of the particle and bumps without rebound into the lower particle's front neighbor. It then begins to slide up the back surface of the particle that it has just bumped.

We first calculate the rate at which momentum is exchanged in directions parallel and perpendicular to the layers. Then we use the fact that in a steady, fully developed flow the ratio of these is constant, in order to determine an expression for the velocity gradient. Upon integrating the velocity gradient, we determine the velocity profile, and, upon averaging the velocity over the depth of the flow, we find a relation between the average velocity and the height of the flow.

II. INCLINED LAYERS

We consider a dense, steady, inclined flow of layers of identical spheres with diameter d and mass m down a slope at an angle θ to the horizontal under the gravitational acceleration g (see Fig. 2). The edges of the spheres are separated by a distance s , and they flow over a rigid bumpy boundary that consists of spheres identical to those of the flow centered on an inclined plane. The flow with thickness H is assumed to consist of layers; so, in terms of the coordinate y transverse to the flow and directed upward with its origin at the basal plane, the number n of spheres in a vertical column above y is, approximately, $n(y) = (H - y)/(d \cos \theta)$.

We denote the angle between a line normal to the incline and the line of centers of a sphere that has fallen between two spheres of the layer below by β . Then

$$\sin \beta = \frac{d + s}{2d}. \quad (2)$$

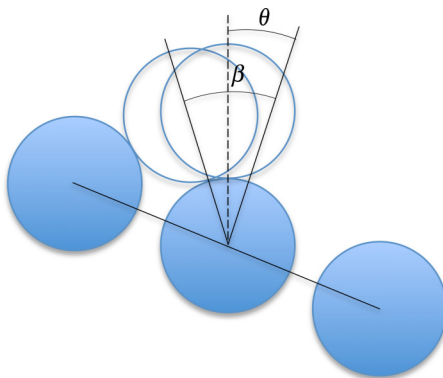


FIG. 3. The rise of a sphere above the layer below, with the line by centers rotated by an angle $\beta - \theta$ between the two.

As the upper sphere moves along the upstream surface of the sphere below, the angle χ between the line of centers and the perpendicular to the layer varies from β to 0 (see Fig. 3). The component N of the weight of the column along the line of centers of two contacting spheres is then

$$N = mgn \cos(\chi - \theta) = mg \frac{(H - y) \cos(\chi - \theta)}{d \cos \theta}. \quad (3)$$

The height h through which the sphere of the layer above falls, before colliding with a sphere of the layer below, is given by

$$h = d[1 - \cos(\theta + \beta)] \approx \frac{1}{2}d(\theta + \beta)^2, \quad (4)$$

where the approximation for small angles is employed. If we neglect friction during the falling of a sphere, the speed v at which the sphere above strikes the sphere below is

$$v = (2gh)^{1/2} = \{2gd[1 - \cos(\theta + \beta)]\}^{1/2} \approx (gd)^{1/2}(\theta + \beta). \quad (5)$$

Then the force on a sphere is the sum of the rate at which impulses \mathcal{N} are transmitted by bumps that occur at a frequency f and the average of the normal force over its upstream surface. The frequency of bumping is taken to be the y derivative u' of the average flow velocity u . The transfer of momentum to a sphere in a bump is assumed to be due to the fall of the column of spheres above it. We assume first that this fall is not resisted by the spheres that neighbor the column and that there is no rebound after the bump. In this case, the impulse is

$$\mathcal{N} = mnv = m \frac{(H - y)}{d \cos \theta} \{2gd[1 - \cos(\theta + \beta)]\}^{1/2} \approx m(H - y) \left(\frac{g}{d}\right)^{1/2} (\theta + \beta). \quad (6)$$

The fact that the impulse is dominated by the velocity of fall, rather than the velocity du' at which the spheres fly between bumps, distinguishes the momentum transfer from that of the μ - I rheology.

We consider next the influence of the geometry of the layer on the transfer of momentum along it. The component of the contact force parallel to the layer is $N \sin \chi$. If this is averaged by integrating from 0 to β and divided by β , the average component of the contact force parallel to the layer is

$$mg \frac{(H - y)}{d} \frac{1}{4\beta} [1 - \cos 2\beta + \tan \theta (2\beta - \sin 2\beta)] \approx mg \frac{(H - y) \beta}{d} \frac{1}{2}. \quad (7)$$

Similarly, the average component of the contact force normal to the layer is

$$mg \frac{(H - y)}{d} \frac{1}{4\beta} [2\beta + \sin 2\beta + \tan \theta (1 - \cos 2\beta)] \approx mg \frac{(H - y)}{d}. \quad (8)$$

Because the bump occurs at a definite point on the sphere, the impulse of the bump involves the geometry, but not an average. The component of the impulse parallel to the layer is

$$\mathcal{N} \sin \beta = m \frac{(H-y)}{d \cos \theta} \{2gd[1 - \cos(\theta + \beta)]\}^{1/2} \sin \beta \approx m \frac{(H-y)}{d} (gd)^{1/2} (\theta + \beta) \beta. \quad (9)$$

With these, the component of the total force \bar{S} parallel to the layer is

$$\begin{aligned} \bar{S} &= \left\{ \frac{1}{4\beta} [(1 - \cos 2\beta) \cos \theta + (2\beta - \sin 2\beta) \sin \theta] + \sqrt{2} u' \left(\frac{d}{g} \right)^{1/2} [1 - \cos(\theta + \beta)]^{1/2} \sin \beta \right\} \\ &\quad \times mg \frac{(H-y)}{d \cos \theta} \\ &\approx mg \frac{(H-y)}{d} \left[\frac{1}{2} + u' \left(\frac{d}{g} \right)^{1/2} (\theta + \beta) \right] \beta, \end{aligned} \quad (10)$$

while the component \bar{P} normal to the layer is

$$\begin{aligned} \bar{P} &= \left\{ \frac{1}{4\beta} [(2\beta + \sin 2\beta) \cos \theta + (1 - \cos 2\beta) \sin \theta] + \sqrt{2} u' \left(\frac{d}{g} \right)^{1/2} [1 - \cos(\theta + \beta)]^{1/2} \cos \beta \right\} \\ &\quad \times mg \frac{(H-y)}{d \cos \theta} \\ &\approx mg \frac{(H-y)}{d} \left[1 + u' \left(\frac{d}{g} \right)^{1/2} (\theta + \beta) \right]. \end{aligned} \quad (11)$$

Consequently, at lowest order, the ratio of forces tangential and normal to the layer is

$$\begin{aligned} \frac{\bar{S}}{\bar{P}} &= \frac{[1/2 + u'(d/g)^{1/2}(\theta + \beta)]\beta}{1 + u'(d/g)^{1/2}(\theta + \beta)} = [1/2 + u'(d/g)^{1/2}(\theta + \beta)]\beta [1 - u'(d/g)^{1/2}(\theta + \beta)] \\ &= \frac{1}{2} [1 + u'(d/g)^{1/2}(\theta + \beta)]\beta; \end{aligned} \quad (12)$$

so

$$u' = \frac{\bar{S}/\bar{P} - \beta/2}{(\theta + \beta)\beta/2} \left(\frac{g}{d} \right)^{1/2}. \quad (13)$$

In a steady fully developed shearing flow, the ratio of shear stress to normal stress is a constant. We express this in terms of the ratio of the tangential and normal forces: $\bar{S}/\bar{P} = \tan \theta \approx \theta$. Using this in Eq. (13) gives

$$u' = \frac{\theta - \beta/2}{(\theta + \beta)\beta/2} \left(\frac{g}{d} \right)^{1/2}, \quad (14)$$

leading to

$$u = \frac{\theta - \beta/2}{(d/g)^{1/2}(\theta + \beta)\beta/2} y. \quad (15)$$

Here and from this point on, we work exclusively with the approximate forms for small angles β and θ . This permits an easier appreciation of the structure of the theory. In fact, neither θ nor β may be small, but the exact forms might be constructed from those already provided.

Sliding friction may be included in this expression, although numerical simulations indicate that in dense, inclined flows the direction of sliding at contacts is not always in the direction of the average flow (e.g., Fig. 15 in Ref. [55]). Assuming that all contacts are sliding in this direction, the

average of the component of the friction force along the layer is $\mu\bar{P}$, while the frictional component of the impulse along the layer is $\mu\mathcal{N}\cos\beta\approx\mu\mathcal{N}$, so

$$\bar{S} = \bar{P} \left\{ \frac{1}{2}\beta + \mu + \left[\frac{(\theta + \beta)}{2} + \mu \right] \beta u' \left(\frac{d}{g} \right)^{1/2} \right\} \quad (16)$$

and

$$u' = \frac{\theta - (\beta/2 + \mu)}{[(\theta + \beta)/2 + \mu]\beta} \left(\frac{g}{d} \right)^{1/2}. \quad (17)$$

The shear rate expressed in Eq. (17) is again a constant, leading to a linear expression for the velocity profile

$$u = \frac{\theta - (\mu + \beta/2)}{[(\theta + \beta)/2 + \mu]\beta(d/g)^{1/2}} y \quad (18)$$

and the average velocity

$$U \equiv \frac{1}{H} \int_0^H u(y) dy = \frac{\theta - (\mu + \beta/2)}{[(\theta + \beta)/2 + \mu]\beta(d/g)^{1/2}} \frac{H}{2}. \quad (19)$$

This model predicts a linear velocity profile, a range of possible angles of inclination, $(\mu + \beta/2) < \theta$, and the scaling of the average velocity with friction, inclination, and depth of flow. The linear dependence on the angle of inclination is that which is observed in the physical experiments and numerical simulations of Sec. III. In contrast, Bagnold's [56] model of collisional momentum exchange would result in a quadratic dependence of the tangential force on the shear rate, and, as a consequence, the average velocity would depend upon the square root of the inclination. In the derivation, we have assumed that the layering and the force chains extend through the entire depth of the flow. However, in many situations, this is not the case, and regions of colliding, rather than contacting, particles exert a collisional pressure on the tops of the force chains. In such flows the linear velocity profile is limited to the layered particles and a collisional velocity profile above it.

The numerical simulations and experiments (e.g., Ref. [46]) indicate that as the distance from the bottom of the flow increases, a point is reached at which the interactions between spheres become so strong that the layering breaks down and random collisions, rather than rubbing and bumping, begin to dominate the transfer of momentum. Consequently, above this point, expressions for the shear stress and pressure from extended or classical kinetic theories for collisional grain flows (e.g., Ref. [57]) may be employed. At the point of transition, the values of the stresses of the layered and collisional models must agree.

The fluctuations in velocity between spheres in two neighboring layers are assumed to be dominated by the downward component of the vertical velocity, $v \approx (gd)^{1/2}(\beta + \theta)$. This velocity fluctuation may be employed to define a two-dimensional (2D) granular temperature T that increases as the number y/d of layers is traversed upwards, due to the accumulation of velocity fluctuations from the layers below:

$$T = \frac{1}{2}g(\beta + \theta)^2 y. \quad (20)$$

Equation (20) describes a linear profile for the granular temperature, which vanishes near a rigid or particle bed and reaches its maximum at the free surface.

In deriving this simple theory, we implicitly assumed that, after each fall, a particle would bump in the lowest possible point against the layer below, with the line of centers forming an angle β with the normal to the flow. However, because of the combined effects of falling and flying, each particle moves along a trajectory, which might result in an effective angle at contact, β_{eff} , smaller than β (see Fig. 4). The flow velocity of the particle relative to the layer below, $u'd$, and the downward

DENSE, LAYERED, INCLINED FLOWS OF SPHERES

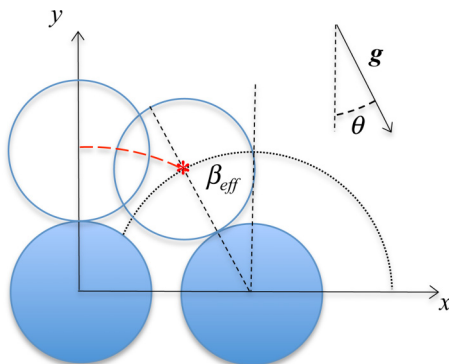


FIG. 4. Trajectory of a particle (red, dashed line) as a result of flying and falling; the red star indicates the coordinate of the center at the moment of bumping against a particle of the layer below. The effective angle at contact is $\beta_{\text{eff}} < \beta$.

velocity due to the gravitational acceleration, g , result in the following trajectory in coordinates system represented in Fig. 4:

$$\frac{y}{d} = 1 - \frac{\hat{t}^2}{4} \left(\frac{x}{d} \right)^2, \quad (21)$$

where $\hat{t} = (2g/d)^{1/2}/u'$ is the ratio of fly, $1/u'$, to fall, $(2g/d)^{-1/2}$, times. We assume that the ratio of fly time to fall time is small.

Flow in three dimensions is more complex but, in our view, not qualitatively different. Spheres are likely to seek out paths between, rather than over, spheres in a layer. However, such paths also involve rubbing, rising, falling, and bumping, albeit to a lesser degree.

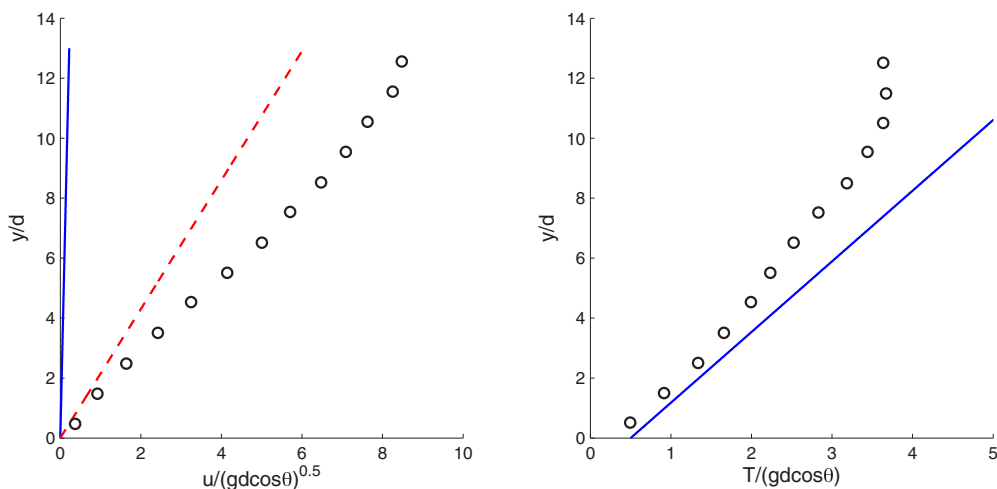


FIG. 5. Comparison of the predicted velocity with [solid blue line, Eq. (18)] and without friction [dashed red line, Eq. (15)] and temperature [solid blue line, Eq. (20)] profiles and those measured in the experiments in Ref. [14] (black circles) shown in Fig. 12 there. The parameters employed are $d = 3$ mm, $\theta = 21^\circ$, $\mu = 0.1$, $\beta = \pi/6$.

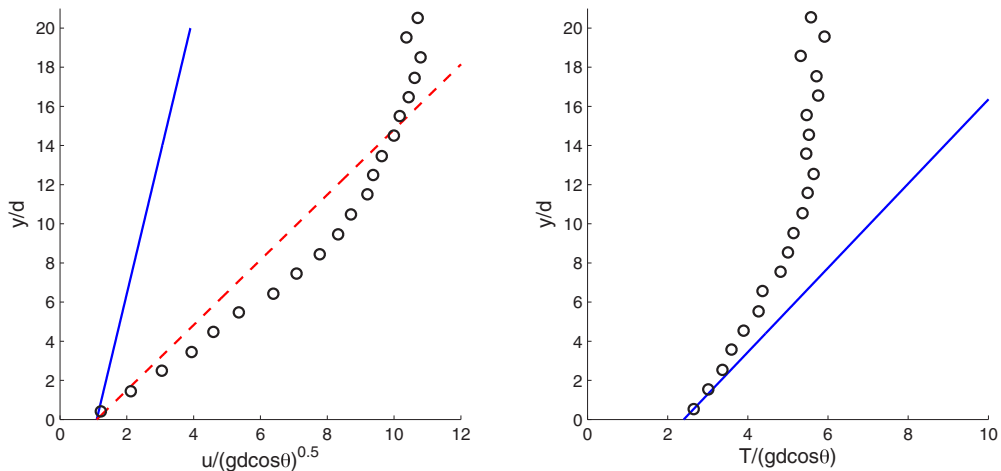


FIG. 6. Comparison of the predicted velocity with [solid blue line, Eq. (18)] and without friction [dashed red line, Eq. (15)] and temperature [solid blue line, Eq. (20)] profiles and those measured in the experiments in Ref. [14] (black circles) shown in Fig. 3 there. The parameters employed are $d = 3$ mm, $\theta = 23^\circ$, $\mu = 0.1$, $\beta = \pi/6$.

III. COMPARISONS WITH EXPERIMENTS AND NUMERICAL SIMULATIONS

We apply the model to those flows that we know of in which there is direct evidence of layers and/or the temperature increases with height. The model may not apply to all of the flows that we test it against. We note that in making comparisons we neglect the sidewall friction. Assuming that the particles of the flow that are in contact with walls separated by a distance W slide with a friction coefficient μ_w , $\tan \theta$ is effectively diminished by an amount $\mu_w H/W$. This would reduce the slope of the velocity curve. We are aware that local inhomogeneities in the stress field can play a role in the local response of the material, but at this stage, we neglect their influence. Finally, we note that in some of the experiments we will consider [2,14,46,58], the ratio between the velocity of fall $(gd)^{1/2}(\theta + \beta)$, given by Eq. (5), and the velocity du' at which the spheres fly between bumps is not

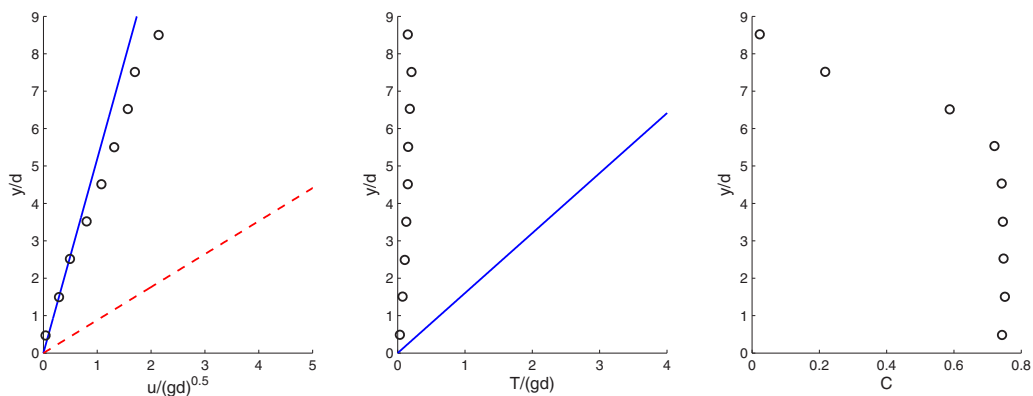


FIG. 7. Comparison of the predicted velocity with [solid blue line, Eq. (18)] and without friction [dashed red line, Eq. (15)] and temperature [solid blue line, Eq. (20)] profiles and those measured in the experiments in Ref. [58] (black circles). The parameters employed are $d = 8$ mm, $\theta = 34^\circ$, $\mu = 0.2$, $\beta = \pi/5.5$.

DENSE, LAYERED, INCLINED FLOWS OF SPHERES

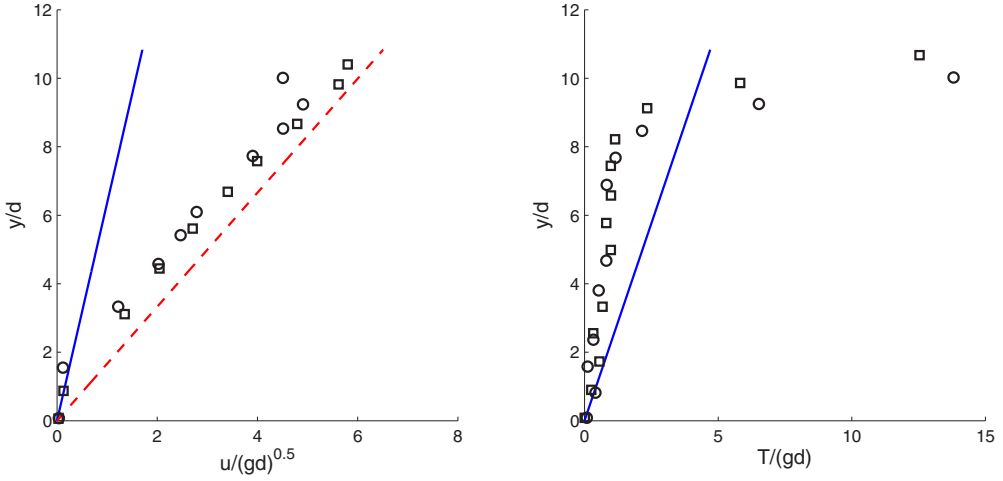


FIG. 8. Comparison of the predicted velocity with [solid blue line, Eq. (18)] and without friction [dashed red line, Eq. (15)] and temperature [solid blue line, Eq. (20)] profiles and those measured in the experiments in Ref. [2] at a slope angle of 21.2° (black circles) and 23.4° (black squares). The parameters employed are $d = 3$ mm, $\theta = 23.4^\circ$, $\mu = 0.1$, $\beta = \pi/6$.

strictly small. It may assume values up to about 0.5, but we consider this a legitimate approximation within the simplified theory we are proposing.

In Fig. 5 we compare the predicted profiles for the particle velocity and for the granular temperature with the experimental measurements of Azanza et al. [14] for $d = 3$ mm, $\theta = 21^\circ$, $\mu = 0.1$, $\beta = \pi/6$. They introduced spheres in a flume with a width slightly larger than the particle diameter, obtaining 2D flows over a rigid bed in a 2D configuration. Although their flows seem to be collisional, the narrow channel width induces layering, and the theory we propose seems to capture the shape of both the velocity and temperature profiles. We slightly underestimate the velocity, probably due to the lower flow resistance in collisional flows. The simpler expression for the velocity profile given in Eq. (15), which does not account for the sliding friction, provides a better prediction of experimental data than Eq. (18). This is consistent with the results of numerical

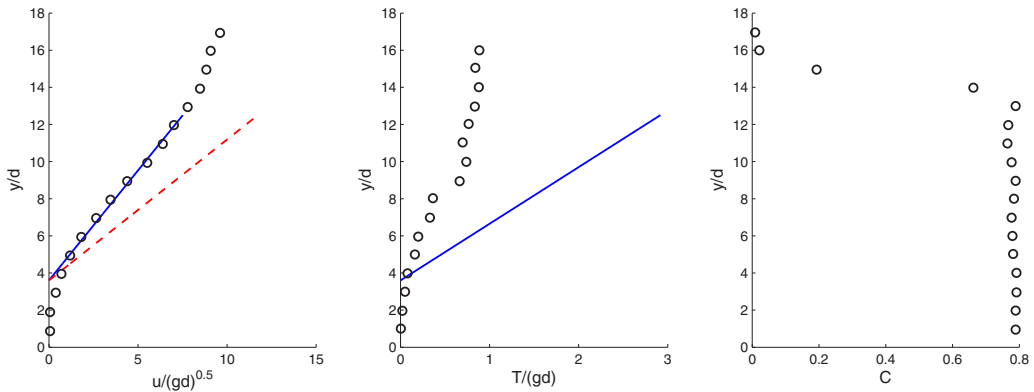


FIG. 9. Comparison of the predicted velocity with [solid blue line, Eq. (18)] and without friction [dashed red line, Eq. (15)] and temperature [solid blue line, Eq. (20)] profiles and those measured in the experiments in Ref. [46] (black circles) shown in Fig. 21 there. The parameters employed are $d = 2$ mm, $\theta = 35.7^\circ$, $\mu = 0.09$, $\beta = \pi/6$, $\omega = 6$ r.p.m.

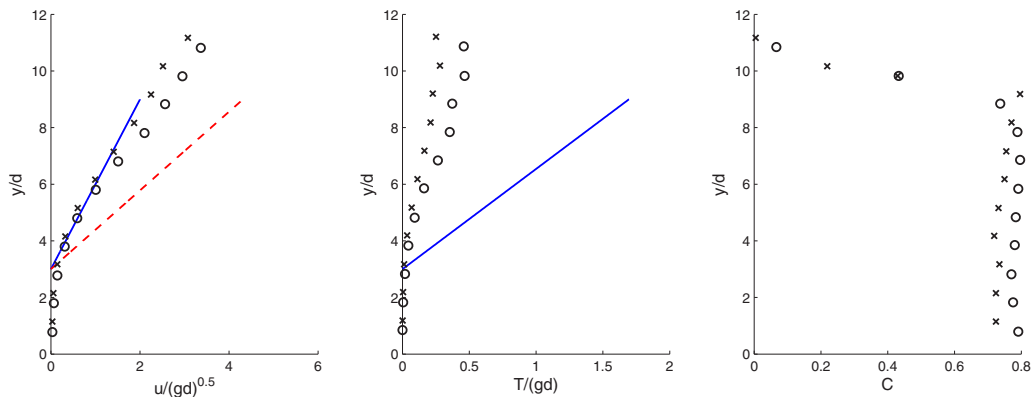


FIG. 10. Comparison of the predicted velocity with [solid blue line, Eq. (18)] and without friction [dashed red line, Eq. (15)] and temperature [solid blue line, Eq. (20)] profiles and those measured in the experiments in Ref. [46] shown in Fig. 24 there for two drum widths: $W/d = 3.33$ (black circles) and $W/d = 6.66$ (black crosses). The other parameters employed are $d = 3$ mm, $\theta = 26.3^\circ$, $\mu = 0.09$, $\beta = \pi/6$, $\omega = 3$ r.p.m.

simulations that show a significant decrease in sliding friction as a function of the orientation of the contact (e.g., Ref. [55]). The prediction for the granular temperature is relatively good.

In Fig. 6 we provide a similar comparison, but for a larger slope, $\theta = 23^\circ$. Because of the greater slip velocity at the base, collisional interactions and the velocity fluctuations are increased. This increase is not incorporated in the model. The slope of the granular temperature profile is slightly overestimated.

In Fig. 7, we compare the predicted profiles of flow velocity and granular temperature with the data of Berton *et al.* [58]. The prediction of the flow velocity is in good agreement with the experimental data, while the granular temperature is, in this case, dramatically overestimated. In this and subsequent figures, we also show the measured concentration profiles, to indicate the extent of regions of greater and lesser concentration.

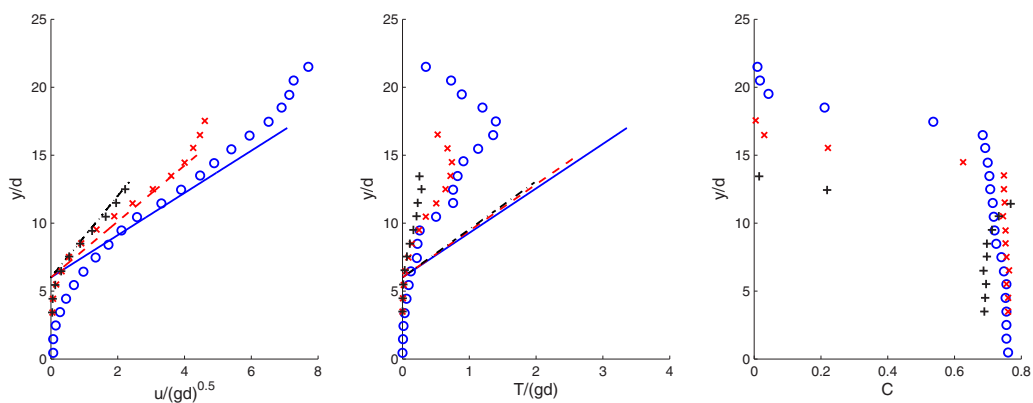


FIG. 11. Comparison of the predicted velocity [Eq. (18)] and temperature [Eq. (20)] profiles for three different particle diameters (solid blue lines for $d_1 = 1$ mm, dashed red lines for $d_2 = 2$ mm, and black dash-dotted lines for $d_3 = 3$ mm) and those measured in the experiments in Ref. [46] shown in Fig. 23 there (blue o for $d_1 = 1$ mm, red x for $d_2 = 2$ mm, and black + for $d_3 = 3$ mm). The other parameters employed are $\theta_1 = 32.0^\circ$, $\theta_2 = 29.1^\circ$, $\theta_3 = 26.3^\circ$, $\mu = 0.09$, $\beta = \pi/6$, $\omega = 3$ r.p.m.

DENSE, LAYERED, INCLINED FLOWS OF SPHERES

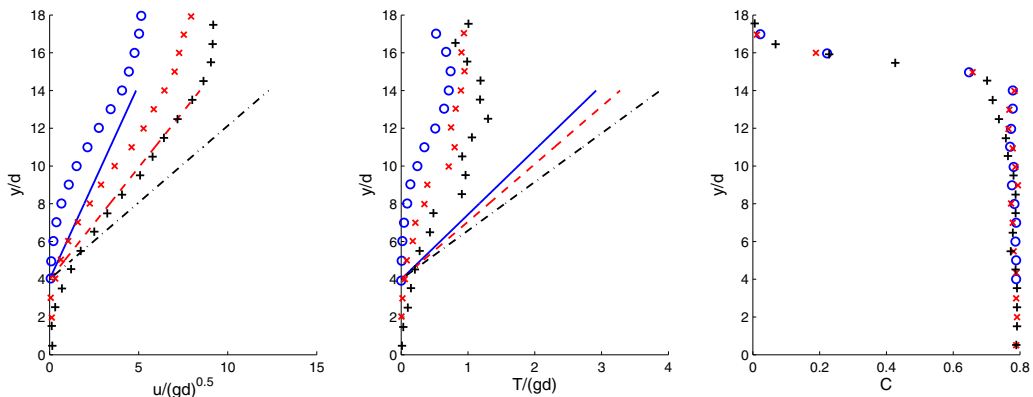


FIG. 12. Comparison of the predicted velocity [Eq. (18)] and temperature [Eq. (20)] profiles for three different rotation speeds of the cylinder (solid blue lines for $\omega_1 = 3$ r.p.m., dashed red lines for $\omega_2 = 6$ r.p.m. and black dash-dotted lines for $\omega_3 = 9$ r.p.m.) and those measured in the experiments in Ref. [46] shown in Fig. 22 there (blue o for $\omega_1 = 3$ r.p.m., red x for $\omega_2 = 6$ r.p.m., and black + for $\omega_3 = 9$ r.p.m.). The other parameters employed are $\theta_1 = 29.1^\circ$, $\theta_2 = 35.7^\circ$, $\theta_3 = 42.8^\circ$, $\mu = 0.09$, $\beta = \pi/6$, $d = 2$ mm.

In Fig. 8 we compare velocity and temperature profiles measured in numerical simulations and experiments in Ref. [2] with the prediction of the theory. As with the data in Ref. [14], there is good agreement for the flow velocity when adopting Eq. (15), with the neglect of sliding friction. The granular temperature is underestimated in the upper layers, where collisional interactions may dominate. In their numerical simulations, Hanes and Walton [2] see that the gradient of the granular temperature reverses direction, moving from the sidewall to the center of the flow. However, the agreement with the prediction of Eq. (20) suggests that the fall-bump mechanism is active near the sidewalls.

In Fig. 9 we compare velocity and temperature profiles measured in the experiments in a quasi-2D rotating drum in Ref. [46], as shown in Fig. 21 there, with the prediction of the theory. The particles employed have a diameter $d = 2$ mm, the drum is rotated at an angular velocity $\omega = 6$ r.p.m, leading to a slope of the flow $\theta = 35.7^\circ$, and the friction coefficient is $\mu = 0.09$. The bumpiness is assumed to be $\beta = \pi/6$. The position of the origin is determined by a linear fit to the velocity. There is good agreement for the velocity, while the granular temperature is underestimated by about a factor of three.

In two dimensions, the fluctuations are accumulated layer by layer; however, in three dimensions, this accumulation is less precise and more diffuse. The influence of the third dimension can be seen in the experimental data shown in Fig. 10, in which the width of the drum is varied: $W/d = 3.33$ and $W/d = 6.66$. The particles have a diameter $d = 3$ mm, and the drum is rotated in both cases at $\omega = 3$ r.p.m. In the narrower drum, in which the width is limited to about three particle diameters, the granular temperature is larger, although the other parameters in the experiment are kept constant.

In Fig. 11 we show how the predictions of the model depend on the particle diameter, when the other parameters are kept constant, and compare with the experimental measures in Ref. [46]. Figure 12 shows the dependence of results on the rotation speed of the cylinder. In both cases, the theory correctly reproduces the tendencies shown in the experiments.

IV. CONCLUSIONS

We have indicated how the presence of gravity can modify the collisional scaling of the stress that was introduced by Bagnold. In a dense flow down an incline, gravity permits an exchange of momentum in weak collisions between spheres that is independent of the shear rate. Then, in addition to a part that is associated with a geometric resistance to sliding, the shear stress contains a

contribution that is linear, not quadratic, in shear rate. Consequently, the profile of average velocity is linear.

Also, because the flow is so dense, we assume that particle motions normal to the flow involve the lifting of columns of particles, and it is the fall of these columns that contributes to the exchange of momentum. As a consequence, the shear stress at a given point of the flow depends explicitly upon height of the material above it, and, in this sense, the stress relation is nonlocal.

Finally, fluctuations in velocity are associated with the motion of spheres perpendicular to the layers. Because the layers are connected, these fluctuations accumulate with distance above the base, resulting in a linearly increasing temperature.

We have introduced a number of situations in which the velocity and temperature profiles exhibit such features, at least through a portion of the depth of the flow. Such flows are often influenced by sidewalls, whose presence seems to promote the existence of layers. In any case, the elements of the model should be accessible to tests in discrete-element simulations. Of particular interest, would be the characterization of the transition between the layered and the random collisional regimes and the relation between the angle β and the volume fraction.

ACKNOWLEDGMENTS

The authors would like to thank Professor Kimberly Hill at the University of Minnesota for valuable discussions. The authors are grateful to the School of Civil and Environmental Engineering at Cornell University, to the Faculty of Science and Technology at the Free University of Bozen-Bolzano, and to the Department of Civil, Environmental and Mechanical Engineering at the University of Trento for their financial support and hospitality.

-
- [1] O. Pouliquen, Scaling laws in granular flows down rough inclined planes, *Phys. Fluids* **11**, 542 (1999).
 - [2] D. M. Hanes and O. R. Walton, Simulations and physical measurements of glass spheres flowing down a bumpy incline, *Powder Tech.* **109**, 133 (2000).
 - [3] B. Andreotti and S. Douady, Selection of velocity profile and flow depth in granular flows, *Phys. Rev. E* **63**, 031305 (2001).
 - [4] C. Ancey, Dry granular flows down an inclined channel: Experimental investigations on the frictional-collisional regime, *Phys. Rev. E* **65**, 011304 (2001).
 - [5] B. Andreotti, A. Daerr, and S. Douady, Scaling laws in granular flows down a rough plane, *Phys. Fluids* **14**, 415 (2002).
 - [6] C. Goujona, N. Thomas, and B. Dalloz-Dubrujeaud, Monodisperse dry granular flows on inclined planes: Role of roughness, *Eur. Phys. J. E* **11**, 147 (2003).
 - [7] GDR MiDi, On dense granular flows, *Eur. Phys. J. E* **14**, 341 (2004).
 - [8] P. Jop, Y. Forterre, and O. Pouliquen, A constitutive law for dense granular flows, *Nature (London)* **441**, 727 (2006).
 - [9] W. Bi, R. Delannay, P. Richard, and A. Valance, Experimental study of two-dimensional, monodisperse, frictional-collisional granular flows down an inclined chute, *Phys. Fluids* **18**, 123302 (2006).
 - [10] S. S. Shirsath, J. T. Padding, N. G. Deen, H. J. H. Clercx, and J. A. M. Kuipers, Experimental study of monodisperse granular flow through an inclined rotating chute, *Powder Tech.* **246**, 235 (2013).
 - [11] T. G. Drake, Structural features in granular flows, *J. Geophys. Res.* **95**, 8681 (1990).
 - [12] T. G. Drake, Granular flow: Physical experiments and their implications for microstructural theories, *J. Fluid Mech.* **225**, 121 (1991).
 - [13] E. Azanza, Ecoulements granulaires bidimensionnels sur un plan incliné, Ph.D. thesis, Ecole Nationale des Ponts et Chaussées (1998).

- [14] E. Azanza, F. Chevoir, and P. Moucheront, Experimental study of collisional granular flows down an inclined plane, *J. Fluid Mech.* **400**, 199 (1999).
- [15] J. A. Dijkstra, F. Rietz, K. A. Lőrincz, M. van Hecke, and W. Losert, Refractive index matched scanning of dense granular materials, *Rev. Sci. Instr.* **83**, 011301 (2012).
- [16] W. Ni and H. Capart, Cross-sectional imaging of refractive-index-matched liquid-granular flows, *Exp. Fluids* **56**, 163 (2015).
- [17] B. Spinewine, H. Capart, M. Larcher, and Y. Zech, Three-dimensional Voronoï imaging methods for the measurement of near-wall particulate flows, *Exp. Fluids* **34**, 227 (2003).
- [18] B. Spinewine, H. Capart, L. Fraccarollo, and M. Larcher, Laser stripe measurements of near-wall solid fraction in channel flows of liquid-granular mixtures, *Exp. Fluids* **50**, 1507 (2011).
- [19] D. Ertas, G. S. Grest, T. C. Halsey, D. Levine, and L. E. Silbert, Gravity-driven dense granular flows, *Europhys. Lett.* **56**, 214 (2001).
- [20] L. E. Silbert, D. Ertas, G. S. Grest, T. C. Halsey, D. Levine, and S. J. Plimpton, Granular flow down an inclined plane: Bagnold scaling and rheology, *Phys. Rev. E* **64**, 051302 (2001).
- [21] F. Chevoir, M. Prochnow, J. T. Jenkins, and P. Mills, Dense granular flows down an inclined plane, in *Powders and Grains 2001*, edited by Y. Kishino (Balkema, Rotterdam, 2001), p. 373.
- [22] N. Mitarai and H. Nakanishi, Velocity correlations in dense granular shear flows: Effects on energy dissipation and normal stress, *Phys. Rev. E* **75**, 031305 (2007).
- [23] K. A. Reddy and V. Kumaran, Dense granular flow down an inclined plane: A comparison between the hard particle model and soft particle simulations, *Phys. Fluids* **22**, 113302 (2010).
- [24] C. Campbell, Clusters in dense-inertial granular flows, *J. Fluid Mech.* **687**, 341 (2011).
- [25] S. Chialvo, J. Sun, and S. Sundaresan, Bridging the rheology of granular flows in three regimes, *Phys. Rev. E* **85**, 021305 (2012).
- [26] V. Kumaran and S. Bharathraj, The effect of base roughness on the development of a dense granular flow down an inclined plane, *Phys. Fluids* **25**, 070604 (2013).
- [27] T. Weinhart, R. Hartkamp, A. R. Thornton, and S. Luding, Coarse-grained local and objective continuum description of three-dimensional granular flows down an inclined surface, *Phys. Fluids* **25**, 070605 (2013).
- [28] C. Campbell, Clusters in dense-inertial granular flows: Two new views of the conundrum, *Gran. Matt.* **16**, 621 (2014).
- [29] P. Mills, D. Loggia, and M. Tixier, Model for a stationary dense granular flow along an inclined wall, *Europhys. Lett.* **45**, 733 (1999).
- [30] P. Mills, M. Tixier, and D. Loggia, Influence of roughness and dilatancy for dense granular flow along an inclined wall, *Eur. Phys. J. E* **1**, 5 (2000).
- [31] D. L. Henann and K. Kamrin, A predictive, size-dependent continuum model for dense granular flows, *Proc. Natl. Acad. Sci. USA* **110**, 6730 (2013).
- [32] K. Kamrin and D. L. Henann, Nonlocal modeling of granular flows down inclines, *Soft Matter* **11**, 179 (2015).
- [33] J. T. Jenkins and D. Berzi, Dense inclined flows of inelastic spheres: Tests of an extension of kinetic theory, *Gran. Matt.* **12**, 151 (2010).
- [34] B. Ö. Arnarson and J. T. Jenkins, Binary mixtures of inelastic spheres: Simplified constitutive theory, *Phys. Fluids* **16**, 4543 (2004).
- [35] M. Larcher and J. T. Jenkins, The evolution of segregation in dense inclined flows of binary mixtures of spheres, *J. Fluid Mech.* **782**, 405 (2015).
- [36] J. T. Jenkins, Dense shearing flows of inelastic disks, *Phys. Fluids* **18**, 103307 (2006).
- [37] J. T. Jenkins, Dense inclined flows of inelastic spheres, *Gran. Matt.* **10**, 47 (2007).
- [38] C. Ancey and P. Evesque, Frictional-collision regime for granular frictional-collision regime for granular suspension flows down an inclined channel, *Phys. Rev. E* **62**, 8349 (2000).
- [39] G. Lois, A. Lemaître, and J. M. Carlson, Emergence of multi-contact interactions in contact dynamics simulations of granular shear flows, *Europhys. Lett.* **76**, 318 (2006).
- [40] C. Campbell, Granular material flows—An overview, *Powder Tech.* **162**, 208 (2006).
- [41] Y. Forterre and O. Pouliquen, Flows of dense granular media, *Annu. Rev. Fluid Mech.* **40**, 1 (2008).

- [42] O. Pouliquen and Y. Forterre, A non-local rheology for dense granular flows, *Phil. Trans. R. Soc. A* **367**, 5091 (2009).
- [43] J. Estep and J. Dufek, Discrete element simulations of bed force anomalies due to force chains in dense granular flows, *J. Volcan. Geothermal. Res.* **254**, 108 (2013).
- [44] L. E. Silbert, G. S. Grest, S. J. Plimpton, and D. Levine, Boundary effects and self-organization in dense granular flows, *Phys. Fluids* **14**, 2637 (2002).
- [45] G. Felix, V. Falk, and U. D’Ortona, Granular flows in a rotating drum: The scaling law between velocity and thickness of the flow, *Eur. Phys. J. E* **22**, 25 (2007).
- [46] A. V. Orpe and D. V. Khakhar, Rheology of surface granular flows, *J. Fluid Mech.* **571**, 1 (2007).
- [47] D. V. N. Prasad and D. V. Khakhar, Granular flow in rotating cylinders with noncircular cross sections, *Phys. Rev. E* **77**, 041301 (2008).
- [48] K. M. Hill and J. Zhang, Kinematics of densely flowing granular mixtures, *Phys. Rev. E* **77**, 061303 (2008).
- [49] K. M. Hill and D. S. Tan, Segregation in dense sheared flows: Gravity, temperature gradients, and stress partitioning, *J. Fluid Mech.* **756**, 54 (2015).
- [50] A. Armanini, M. Larcher, and L. Fraccarollo, Intermittency of rheological regimes in uniform liquid-granular flows, *Phys. Rev. E* **79**, 051306 (2009).
- [51] A. Armanini, M. Larcher, M. Dumbser, and E. Nucci, Submerged granular channel flows driven by gravity, *Adv. Water Res.* **63**, 1 (2014).
- [52] A. Armanini, H. Capart, L. Fraccarollo, and M. Larcher, Rheological stratification of liquid-granular debris flows down loose slopes, *J. Fluid Mech.* **532**, 269 (2005).
- [53] M. Larcher, L. Fraccarollo, A. Armanini, and H. Capart, Set of measurement data from flume experiments on steady uniform debris flows, *J. Hydraulic Res.* **45**, 59 (2007).
- [54] L. Fraccarollo, M. Larcher, and A. Armanini, Depth-averaged relations for granular-liquid uniform flows over mobile bed in a wide range of slope values, *Gran. Matt.* **9**, 145 (2007).
- [55] F. da Cruz, S. Emam, M. Prochnow, J. N. Roux, and F. Chevoir, Rheophysics of dense granular materials: Discrete simulation of plane shear flows, *Phys. Rev. E* **72**, 021309 (2005).
- [56] R. A. Bagnold, Experiments on a gravity-free dispersion of large solid spheres in a Newtonian fluid, *Proc. R. Soc. London A* **225**, 49 (1954).
- [57] J. T. Jenkins and D. Berzi, Kinetic theory applied to inclined flows, *Gran. Matt.* **14**, 79 (2012).
- [58] G. Berton, R. Delannay, P. Richard, N. Taberlet, and A. Valance, Two-dimensional inclined chute flows: Transverse motion and segregation, *Phys. Rev. E* **68**, 051303 (2003).